

Contents lists available at [ScienceDirect](http://ScienceDirect)

# Biochimica et Biophysica Acta

journal homepage: [www.elsevier.com/locate/bbamcr](http://www.elsevier.com/locate/bbamcr)

## Attenuation of doxorubicin-induced cardiac injury by mitochondrial glutaredoxin 2<sup>☆</sup>

Nicole M. Diotte<sup>a</sup>, Ye Xiong<sup>a</sup>, Jinping Gao<sup>b</sup>, Balvin H.L. Chua<sup>b</sup>, Ye-Shih Ho<sup>a,\*</sup><sup>a</sup> Institute of Environmental Health Sciences and Department of Biochemistry and Molecular Biology, Wayne State University, 2727 Second Avenue, Room 4000, Detroit, MI 48201, USA<sup>b</sup> Department of Pharmacology and Cecile Cox Quillen Laboratory of Geriatric Research, James H. Quillen College of Medicine, East Tennessee State University; and James H. Quillen Veterans Affairs Medical Center, Johnson City, TN, USA

### ARTICLE INFO

#### Article history:

Received 29 August 2008

Received in revised form 24 October 2008

Accepted 24 October 2008

Available online 6 November 2008

#### Keywords:

Oxidative stress

Protein S-glutathionylation

Transgenic mice

Mitochondria

Cytochrome c

### ABSTRACT

While the cardiotoxicity of doxorubicin (DOX) is known to be partly mediated through the generation of reactive oxygen species (ROS), the biochemical mechanisms by which ROS damage cardiomyocytes remain to be determined. This study investigates whether S-glutathionylation of mitochondrial proteins plays a role in DOX-induced myocardial injury using a line of transgenic mice expressing the human mitochondrial glutaredoxin 2 (Glx2), a thiotransferase catalyzing the reduction as well as formation of protein–glutathione mixed disulfides, in cardiomyocytes. The total glutaredoxin (Glx) activity was increased by 76% and 53 fold in homogenates of whole heart and isolated heart mitochondria of *Glx2* transgenic mice, respectively, compared to those of nontransgenic mice. The expression of other antioxidant enzymes, with the exception of glutaredoxin 1, was unaltered. Overexpression of Glrx2 completely prevents DOX-induced decreases in NAD- and FAD-linked state 3 respiration and respiratory control ratio (RCR) in heart mitochondria at days 1 and 5 of treatment. The extent of DOX-induced decline in left ventricular function and release of creatine kinase into circulation at day 5 of treatment was also greatly attenuated in *Glx2* transgenic mice. Further studies revealed that heart mitochondria overexpressing Glrx2 released less cytochrome c than did controls in response to treatment with tBid or a peptide encompassing the BH3 domain of Bid. Development of tolerance to DOX toxicity in transgenic mice is also associated with an increase in protein S-glutathionylation in heart mitochondria. Taken together, these results imply that S-glutathionylation of heart mitochondrial proteins plays a role in preventing DOX-induced cardiac injury.

© 2008 Elsevier B.V. All rights reserved.

### 1. Introduction

The anthracycline antibiotic doxorubicin (DOX) is one of the most effective anticancer drugs for treating various types of cancers such as carcinomas, soft tissue sarcomas, multiple myeloma, non-Hodgkin's lymphomas, and Hodgkin's disease. However, the therapeutic effectiveness of DOX is greatly restricted by its dose dependent and cumulative cardiotoxic side effects [1–4].

**Abbreviations:** DOX, doxorubicin; ROS, reactive oxygen species; GSH, glutathione; protein–SSG, protein–glutathione mixed disulfides; Glrx1, glutaredoxin 1; Glrx2, glutaredoxin 2; Trx1, thioredoxin 1, Trx2, thioredoxin 2; RCR, respiratory control ratio; P/O ratio, ADP/O ratio; CuZnSOD, copper–zinc superoxide dismutase; MnSOD, manganese superoxide dismutase; Gpx1, glutathione peroxidase 1;  $\alpha$ -MyHC,  $\alpha$ -myosin heavy chain; BCA, bicinchoninic acid; HED, 2-hydroxyethyl disulfide; NEM, N-ethylmaleimide

<sup>☆</sup> The work was supported by American Heart Association Greater Midwest Affiliate grants 0455876Z and 0655631Z, and a pilot grant from NIEHS Center (P30 ES06639) to Y.-S. H.; and by NIH grant HL087271, a grant from the Department of Veterans Affairs Merit Review, and a grant-in-aid from American Heart Association Southeast Affiliate to B.H.L.C. The use of equipment in the Imagine and Cytometry Facility Core was supported by a Center grant P30 ES06639.

\* Corresponding author. Tel.: +1 313 963 7660; fax: +1 313 577 0082.

E-mail address: [yho@wayne.edu](mailto:yho@wayne.edu) (Y.-S. Ho).

The mechanism by which DOX causes myocardial injury is not fully understood. Nonetheless, the free radical hypothesis of DOX toxicity has been steadily gaining support over the years. Following entry into cardiomyocytes, DOX can generate reactive oxygen species (ROS) via two distinct mechanisms. First, it can form a complex with iron(III). The iron subsequently receives one electron from the bounded DOX to generate an iron(II)–DOX free radical complex which can then reduce oxygen and hydrogen peroxide to superoxide anion radical (superoxide) and hydroxyl radical, respectively [5,6]. Second, DOX can also generate ROS through the mechanism of reduction–oxidation (redox) cycling, a reaction that is catalyzed by a number of NAD(P)H oxidoreductases [7–12]. At the subcellular level, mitochondria are believed to be the primary target of DOX-induced cardiotoxicity. The mitochondria of DOX-poisoned heart show morphological abnormalities that are associated with biochemical derangements including inhibition of electron transfer complexes, decrease in efficiency of respiration, and disruption of calcium homeostasis [13–19].

The role of ROS in DOX-induced cardiac toxicity is supported by the findings that treatment of animals with a variety of antioxidants such as probucol, amifostine, dexrazoxane, and melatonin protects heart against the toxicity of DOX [20–24]. Furthermore, overexpression of antioxidant enzymes such as manganese superoxide dismutase (MnSOD), catalase, or glutathione peroxidase 1 (Gpx1) in

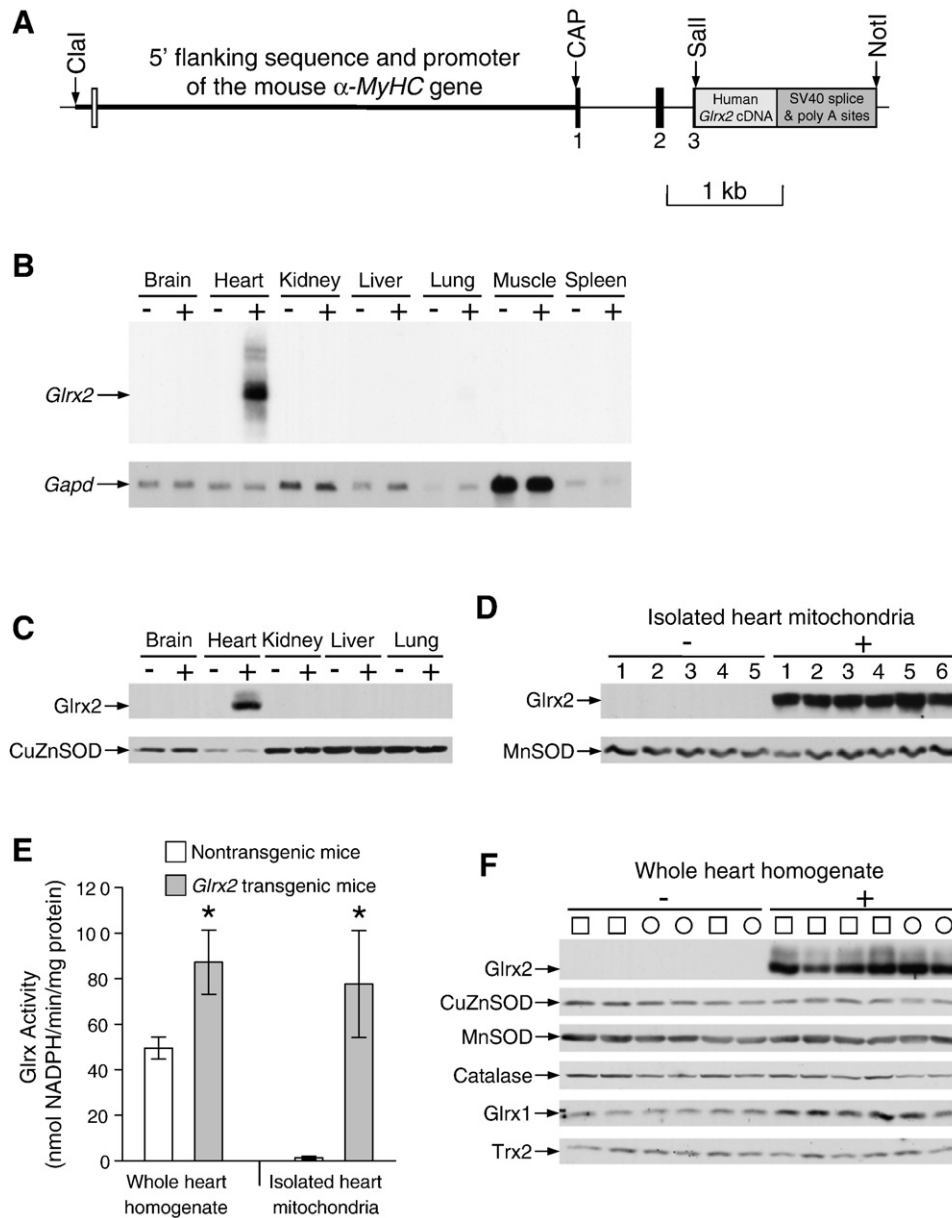


**Fig. 1.** Characterization of the human *Glrx2* transgenic mice. (A) Schematic diagram of the human *Glrx2* transgene. The full-length human *Glrx2* cDNA coding for the mitochondrial *Glrx2* was cloned downstream to a 5.5-kb mouse genomic fragment (namely  $\alpha$ -5.5) which spans from the last intron of the mouse  $\beta$ -*MyHC* gene to the 5' untranslated region of exon 3 of the mouse  $\alpha$ -*MyHC* gene. Open box represents the last noncoding exon of the mouse  $\beta$ -*MyHC* gene. Black boxes represent the first three exons of the mouse  $\alpha$ -*MyHC* gene. The number of the exon of the mouse  $\alpha$ -*MyHC* gene is indicated under each exon. The locations of three unique restriction sites are also indicated in the map. CAP represents transcription initiation site of the mouse  $\alpha$ -*MyHC* gene. (B) RNA blot analysis showing expression of *Glrx2* transgene in heart and lungs of a transgenic mouse. The RNA blot membrane was first hybridized with  $^{32}$ P-labeled human *Glrx2* cDNA and then re-hybridized with a cDNA coding for the rat glyceraldehyde 3-phosphate dehydrogenase (*Gapd*) to determine the variations in sample loading. (C) Protein blot analysis of tissue homogenates showing that the human *Glrx2* protein is specifically expressed in heart of a transgenic mouse. To reveal variations in sample loading, the same blot membrane was re-reacted with antibodies against copper–zinc superoxide dismutase (CuZnSOD). (D) Expression of the human *Glrx2* protein in heart mitochondria of *Glrx2* transgenic mice. Ten micrograms of heart mitochondrial proteins from 5 male nontransgenic mice and 6 male *Glrx2* transgenic mice were separated on a SDS–polyacrylamide gel for blot analysis. Another blot membrane prepared from a gel loaded with the same amounts of samples was reacted with antibodies against manganese superoxide dismutase (MnSOD). (E) Total *Glrx* activity in whole heart homogenates and homogenates of isolated heart mitochondria of nontransgenic and littermate *Glrx2* transgenic mice. Each value represents mean  $\pm$  SD and  $n \geq 5$ . \*,  $p < 0.0001$  compared to the corresponding samples of nontransgenic mice. (F) Expression of antioxidant enzymes in hearts of nontransgenic and *Glrx2* transgenic mice. Thirty micrograms of whole heart homogenates of six individual nontransgenic mice and *Glrx2* transgenic mice were loaded on several gels for blot analysis. The gender is shown on top of the figure. Square and circle represent male and female mice, respectively. In (B), (C), (D), and (F), – and + represent nontransgenic and *Glrx2* transgenic mice, respectively.

cardiomyocytes of transgenic mice greatly attenuates DOX-induced cardiac injury [25–27]. Since MnSOD specifically converts superoxide to  $H_2O_2$  and the other two enzymes decompose  $H_2O_2$ , these studies strongly support the role of ROS in DOX-induced cardiotoxicity. In addition, because MnSOD is only located in the mitochondria, the results also indicate mitochondria as the major target of DOX-induced toxicity in cardiomyocytes.

Although these studies have demonstrated the role of ROS in DOX-induced myocardial injury, the biochemical mechanisms by which ROS damage cardiomyocytes are not understood. Previous studies have shown that protein cysteinyl thiols are among the most susceptible targets of ROS within cells. The cysteine residues of proteins, in the absence of vicinal thiols, can be sequentially oxidized to cysteine sulfenic acids ( $-SOH$ ), sulfinic acids ( $RSO_2H$ ), and sulfonic

(RSO<sub>3</sub>H) acids. In addition, they can react with the vicinal protein thiols and non-protein thiols such as glutathione (GSH) to form intra- and inter-protein disulfides and protein–GSH mixed disulfides (protein–SSG), respectively. Since GSH is the most abundant non-protein thiol in cells (at concentrations between 0.5 and 20 mM) [28], the majority of protein mixed disulfides formed inside cells under oxidative stress is believed to be protein–SSG. S-glutathionylation can have a profound effect on the catalytic and structural functions of proteins. For example, the catalytic functions of transcription factors NF- $\kappa$ B and NF-1 [29,30] protein tyrosine phosphatase 1B [PTP-1B] [31,32], and protein kinase C- $\alpha$  [33] are inactivated by S-glutathionylation. On the other hand, S-glutathionylation enhances the activities of a number of other proteins, such as HIV-1 protease, glutathione S-transferase, and Ras [34–36]. Therefore, the physiological changes due to protein S-glutathionylation as a consequence of cell signaling events or oxidative stress are dependent on which of the effector proteins is S-glutathionylated.

In mammals, the protein–SSG mixed disulfides are predominantly reduced by isoforms of glutaredoxin (Glx) via a monothiol mechanism [37]. Glutaredoxin 1 (Glx1) is a 12-kDa cytosolic protein [38]. Glutaredoxin 2 (Glx2) is expressed from two alternatively spliced mRNAs, resulting in translocation into either the mitochondria or the nucleus [39,40]. Interestingly, Glx is also capable of catalyzing S-glutathionylation of proteins in the presence of a glutathione-thiyl radical generating system [41–43]. Further studies have shown that overexpression of either Glx1 or Glx2 protects cells against injury resulting from oxidative stress [44–49]. However, which of the two catalytic activities of Glx1 and Glx2 contributes to their protective function *in vitro* in cultured cells remains to be determined.

The present study seeks to determine whether S-glutathionylation of mitochondrial proteins in heart plays a role in DOX-induced myocardial injury using a line of transgenic mice overexpressing mitochondrial Glx2 in cardiomyocytes. Our results show that Glx2 overexpression greatly protects mouse heart from DOX-induced mitochondrial and contractile dysfunction, and the protection is associated with an increased S-glutathionylation of mitochondrial proteins.

## 2. Materials and methods

### 2.1. Generation of human Glx2 transgenic mice

To construct the transgene, a full-length cDNA fragment coding for the human mitochondrial Glx2 (IMAGE clone 512859, NCBI accession #AA062724) was isolated from plasmid vector pSK (Stratagene, La Jolla, CA) by digestion with enzymes BamHI and XhoI (the BamHI restriction site is located in the multiple cloning sites of plasmid pSK) and then cloned into the corresponding restriction sites in plasmid pSL1180 (GE Healthcare, Amersham Biosciences Corp, Piscataway, NJ). The human Glx2 cDNA fragment was again isolated from plasmid pSL1180 by digestion with enzymes Sall and XhoI (the Sall restriction site is located in the multiple cloning sites of plasmid pSL1180) and inserted into a previously constructed expression vector at the Sall site, downstream to the 5' flanking sequence and promoter of the mouse  $\alpha$ -myosin heavy chain ( $\alpha$ -MyHC) gene [50]. [The DNA fragment containing the 5' flanking sequence and promoter of the mouse  $\alpha$ -MyHC gene, namely  $\alpha$ -5.5, was originally provided by Dr. Jeff Robbins of University of Cincinnati, Cincinnati, OH [51]. The entire expression sequence (Fig. 1A), including the genomic sequence of the mouse  $\alpha$ -MyHC gene, the human Glx2 cDNA, and the SV40 splice and polyadenylation sites (Fig. 1A), was released from the expression vector by digestion with enzymes ClaI and NotI and purified after separation on an agarose gel. The DNA fragment was then micro-injected into the pronuclei of fertilized eggs harvested from female B6C3 (C57BL/6  $\times$  C3H) F1 mice mated with male B6C3 F1 mice according to the standard method [52]. Only one line of transgenic mice was generated. The mice used in the studies were generated by

breeding the female (hemizygous) transgenic mouse with male B6C3 hybrid mice. Transgenic mice were identified by Southern blot analysis of mouse tail DNA. Both the male and female mice were used in the studies and the nontransgenic littermates were used as controls for transgenic mice.

### 2.2. Preparation of tissue samples for gene expression studies

Total RNA was isolated from tissues of Glx2 transgenic mouse and nontransgenic littermate using the TRIZOL reagent (Invitrogen, Carlsbad, CA) according to the procedures recommended by the manufacturer. Thirty micrograms of total RNA were denatured with glyoxal and subjected to blot analysis according the method described by Thomas [53]. For protein analysis, tissues were homogenized in 1.5 to 2 ml of lysis buffer (50 mM potassium phosphate buffer, pH 7.8, 0.5% Triton X-100, and 3% glycerol) containing protease inhibitor cocktail (P-8340, Sigma, St. Louis, MO) and 1 mM phenylmethylsulfonyl fluoride with a Polytron homogenizer, followed by sonication. The homogenates were then clarified by centrifugation at 20,000  $\times$ g for 15 min and stored at  $-70$  °C. The protein concentration of tissue homogenates was determined by the use of a bicinchoninic acid (BCA) protein assay kit (Pierce, Rockford, IL). Thirty micrograms of tissue proteins were separated on a SDS-polyacrylamide gel for blot analysis. The protein blot membrane was reacted with polyclonal antibodies against the human Glx2 generated in rabbits (kindly provided by Dr. Marjorie Lou of University of Nebraska at Lincoln, Lincoln, NE), and with antibodies against human copper–zinc superoxide dismutase (CuZnSOD), rat manganese superoxide dismutase (MnSOD), bovine catalase, human Glx1, and human thioredoxin 2 (Trx2), followed by the standard procedures of chemiluminescence to visualize the antibody-bound proteins on an X-ray film. The intensities of the signals were quantified using a Kodak Imagine Station 440CF equipped with the Kodak ID Image Analysis Software (Eastman Kodak Company, Rochester, NY).

### 2.3. Enzymatic activity assay for Glx

The method described by Johansson et al. [54] was used to determine the total activity of Glx (including Glx1 and Glx2) in homogenates of mouse hearts and isolated heart mitochondria. Briefly, 10  $\mu$ l of 70 mM 2-hydroxyethyl disulfide (HED) were added to 0.96 ml of reaction mixture containing 100 mM Tris–HCl, pH 8.0, 2 mM EDTA, 0.1 mg/ml bovine serum albumin, 200  $\mu$ M NADPH, 1 mM GSH, and 0.4 U/ml of glutathione reductase, followed by incubation at 30 °C for 3 min. Fifty microliters of diluted heart or mitochondrial homogenate were then added to the reaction mixture to initiate the reaction. The decrease in absorbance at 340 nm was then followed for 30 s using a Shimadzu UV-160U spectrophotometer (Shimadzu Inc., Columbia, MD). The background rates of NADPH oxidation resulting from sample alone (without HED) and HED alone (without sample) were also measured and deducted from the observed decrease of absorbance at 340 nm. The amount of NADPH oxidation in the reaction was calculated using an extinction coefficient of 6.2 mM<sup>-1</sup>cm<sup>-1</sup>. The activity of Glx is defined as nmoles (nmol) of NADPH oxidized in 1 min by 1 mg of protein.

### 2.4. Enzymatic activity assay for glutathione peroxidase and thioredoxin reductase-dependent peroxidase

The glutathione peroxidase activity was measured in a reaction coupled to NADPH oxidation. Sodium azide was added to the reaction mixture to inhibit the activity of catalase [55]. Briefly, 0.1 ml of heart or mitochondrial homogenate were initially mixed with 0.85 ml of reaction mixture (20 mM potassium phosphate buffer, pH 7.0, 0.6 mM EDTA, 0.15 mM NADPH, 2 mM GSH, 1 mM sodium azide, and 4 U/ml of glutathione reductase) at room temperature. The reaction was then initiated by adding 50  $\mu$ l of 2 mM hydrogen peroxide to the reaction

mixture and the decrease in absorbance at 340 nm was followed for 30 s. The activity of glutathione peroxidase was defined as nmoles (nmol) of NADPH oxidized in 1 min by 1 mg of protein at 2 mM GSH.

The thioredoxin-dependent peroxidase activity was measured in a solution of 50 mM Hepes (pH 7.3), 0.12  $\mu$ M recombinant rat thioredoxin reductase (American Diagnostica Inc, Stamford, CT), and 0.2 mM NADPH [56]. The reaction was initiated by addition of H<sub>2</sub>O<sub>2</sub> to a final concentration of 0.25 mM, and the decrease in absorbance at 340 nm was then followed.

### 2.5. Treatment of mice with doxorubicin

Mice of either sex at 8 to 10 weeks of age were injected intraperitoneally with DOX (EMD Biosciences, Inc., La Jolla, CA) dissolved in normal saline at a dose of 22.5 mg/kg or saline alone as control. The mice were then sacrificed at both days 1 and 5 post injection for determining the efficiency of respiration of heart mitochondria, or at day 5 only for measurement of cardiac contractile function *in vivo*.

### 2.6. Isolation of mouse heart mitochondria and measurement of mitochondrial respiratory and phosphorylating activities

Mouse heart mitochondria were isolated and their respiratory and phosphorylating activities measured according to the methods described previously [27]. The purity of mitochondria was evaluated by protein blot analysis using antibodies against lamin B, cytochrome P450 CYP1A1/2, and heat shock protein Hsp90 $\alpha$ , the proteins that are present in the nuclei, microsomes, and cytosol, respectively. None of these antibodies reacted with the proteins prepared from the isolated heart mitochondria (data not shown). Respiratory control ratio (RCR) was calculated as the ratio of state 3 to state 4 respiration. ADP/O ratio (P/O ratio) was determined by dividing the amount (nmoles) of ADP added by the amount (natoms) of oxygen consumed during state 3 respiration.

### 2.7. Activity assay for creatine kinase in serum

Mouse blood was collected by cardiac puncture at the time of sacrifice. The blood was then placed in a microfuge tube and allowed to fully clot on ice for 30 min. The tube was then centrifuged to separate serum from the clot and cell pellet. The activity of creatine kinase in serum was assayed using two commercial kits (Sigma, St. Louis, MO and Diagnostic Chemicals Limited, Charlottetown, PE, Canada) according to the procedures suggested by the manufacturers.

### 2.8. Measurement of *in vivo* cardiac function

At day 5 of saline or DOX treatment, mice were anesthetized with 2% isoflurane and ventilated with room air (at a tidal volume of 0.5 ml and a rate of 110–120 breaths/min) through a tracheostomy cannula that was connected to a rodent respirator (Columbus Instruments International, Columbus, OH). A substernal transverse incision was then made to expose the heart and the inferior vena cava. A microtip pressure–volume catheter (SPR-839; Millar Instruments, Houston, TX) was inserted into the left ventricle through a 25-gauge apical stab wound to allow measurement of the steady state cardiac function. To acutely change the cardiac preload, occlusion of inferior vena cava was produced over a 1-s period. At the completion of study, 10  $\mu$ l of hypertonic saline (15%) were injected into the right atrium to allow calibration of the parallel volume (V<sub>p</sub>). The conductance and pressure signals were continuously recorded at a sampling rate of 1000 s<sup>-1</sup> using an ARIA pressure–volume conductance system (Millar Instruments) that was coupled to a Powerlab/4SP A/D converter (AD Instruments, Mountain View, CA), and then stored and displayed on a computer. Data were recorded as a series of pressure–volume loops and analyzed with a cardiac pressure–volume analysis program (PVAN3.4; Millar Instruments, Houston, TX).

### 2.9. Induction of cytochrome *c* release from isolated heart mitochondria

Release of cytochrome *c* from heart mitochondria was induced with either a 26-mer peptide containing the BH3 domain of Bid (EDIIRNIARHLAQQVGSMDRSIPPGL) or recombinant mouse tBid (Sigma, St. Louis, MO). Briefly, heart mitochondria of nontransgenic and *Glrx2* transgenic mice (containing 0.1 mg of protein) were incubated at 37 °C in 60  $\mu$ l of experimental buffer (125 mM KCl, 10 mM Tris–MOPS, pH 7.4, 1 mM KH<sub>2</sub>PO<sub>4</sub>, 5 mM glutamate, 2.5 mM malate, and 10  $\mu$ M EGTA) as control, or in the same buffer supplemented with a 26-mer peptide encompassing the BH3 domain of Bid (at a final concentration of 50  $\mu$ M) or a recombinant mouse tBid (at a final concentration of 1  $\mu$ M). At 0, 0.5, 1, and 2 h of incubation, a set of tubes was removed from the water bath and the mitochondria were separated by centrifugation at 15,000  $\times$ g for 5 min. The supernatant in each tube was collected and stored under –20 °C until further study. The pellet of mitochondria was dissolved in 75  $\mu$ l of solution containing 10 mM Tris, pH 8.0, 1 mM EDTA, and 1% SDS. The content of cytochrome *c* in these samples was determined by protein blot analysis using a rabbit monoclonal antibody purchased from Cell Signaling Technologies Corp. (Danvers, MA).

### 2.10. Detection of protein S-glutathionylation in heart mitochondria by protein blot analysis

For determining the effect of *Glrx2* overexpression on S-glutathionylation of mitochondria proteins, the minced mouse heart in 3.0 ml of SEE solution (250 mM sucrose, 10 mM Hepes, pH 7.4, 0.5 mM EGTA, 0.5 mM EDTA, and 1.0 mg/ml defatted BSA) containing Nagarse (5 mg/g tissue) was initially subjected to a total of four cycles of homogenization as described previously [27]. The total volume of the heart homogenate was then adjusted to 10 ml with SEE solution containing 30 mM N-ethylmaleimide (NEM) to prevent further S-glutathionylation of proteins during sample manipulation. The same concentration of NEM was also included in the SEE and sucrose solutions that were used in the subsequent washing procedures for isolation of mitochondria. Finally, the pellet of heart mitochondria was re-suspended in 0.3 ml of lysis buffer, as that used for preparation of whole heart homogenate, containing 30 mM NEM, and stored at –70 °C. The suspension of heart mitochondria was then subjected to two cycles of freezing-and-thawing and clarified by centrifugation at 20,000  $\times$ g for 15 min. The supernatant was collected and protein concentration determined by the BCA method. Forty micrograms of soluble proteins of heart mitochondria were then separated on a non-reducing SDS-polyacrylamide gel and transferred to a piece of nitrocellulose membrane. The protein blot membrane was reacted with a monoclonal antibody against GSH (ViroGen, Watertown, MA).

### 2.11. Statistical analysis

For experiments containing more than two groups of samples, the data were first analyzed by one-way analysis of variance (ANOVA), followed by a Newman–Keuls post hoc comparison. The unpaired *t* test was used to analyze the experiments consisting of only two groups of samples. Differences with a *p* value < 0.05 are considered statistically significant.

## 3. Results

### 3.1. Generation and characterization of transgenic mice overexpressing *Glrx2* in mitochondria of cardiomyocytes

To investigate whether the mitochondrial *Glrx2* functions in preventing DOX-induced cardiotoxicity, we generated a line of transgenic mice in which the human *Glrx2* transgene is driven by the 5' flanking sequence and promoter of the mouse  $\alpha$ -MyHC gene



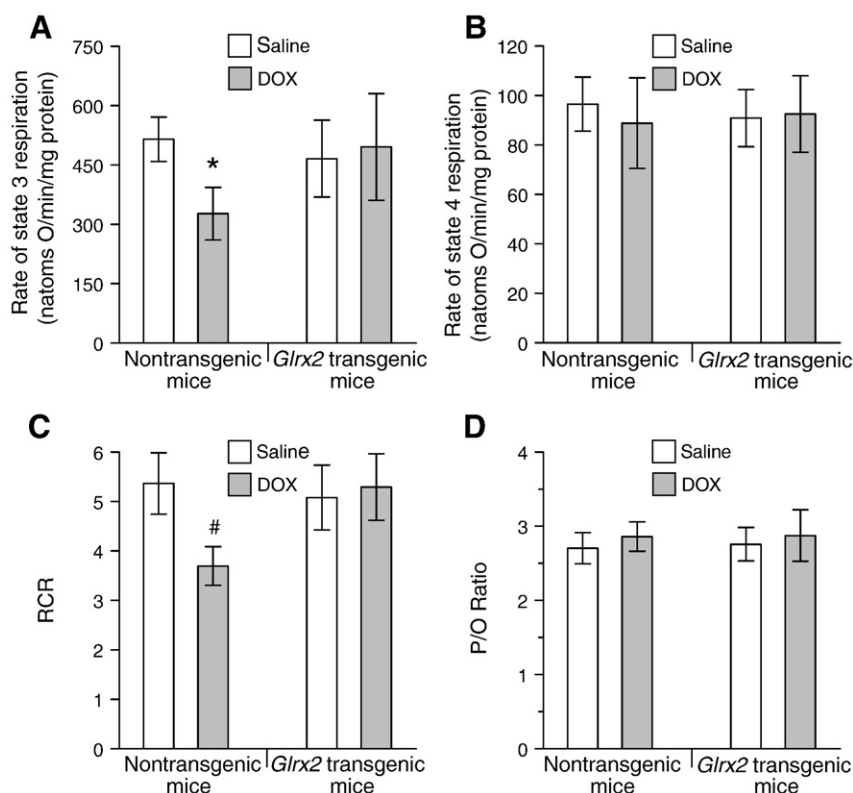


**Fig. 2.** *Glxr2* overexpression prevents DOX-induced decrease in the efficiency of NAD-linked respiration in heart mitochondria at 1 day of treatment. (A) DOX treatment decreases the rate of state 3 respiration in heart mitochondria of nontransgenic mice but not *Glxr2* transgenic mice. (B) The rate of state 4 respiration is not affected by DOX treatment in either nontransgenic or *Glxr2* transgenic mice. (C) The efficiency of NAD-linked oxidative phosphorylation (as determined by the value of RCR) is decreased in heart mitochondria of nontransgenic mice but not littermate *Glxr2* transgenic mice. (D) The P/O ratio of NAD-linked respiration is not affected by DOX treatment in heart mitochondria of either type of mice. Each bar represents mean  $\pm$  SD and  $n=6$  for each experiment. \*,  $p<0.05$  and #,  $p<0.001$  versus heart mitochondria of saline-treated nontransgenic mice.

(Fig. 1A). As shown in Fig. 1B, a species of human *Glxr2* mRNA was found to be highly expressed in heart and to a much lesser extent in lungs of a transgenic mouse (Fig. 1B). Expression of the human *Glxr2* protein in hearts of transgenic mice was demonstrated by protein blot analysis using an antiserum against human *Glxr2* that has a very low affinity for the endogenous mouse *Glxr2* protein (Fig. 1C). However, the human *Glxr2* protein in lungs of transgenic mice was not detectable due to the very low level of mRNA expressed.

Since the human *Glxr2* cDNA contained in the transgene codes for a mitochondrial *Glxr2* protein, expression of the human *Glxr2* protein in heart mitochondria of transgenic mice was further confirmed by protein blot analysis (Fig. 1D). These findings suggest that the human *Glxr2* protein is properly translocated into the mitochondria of transgenic hearts.

We then determined whether the expressed human *Glxr2* is functional. As shown in Fig. 1E, the total *Glxr* activity in whole heart homogenates of transgenic mice was increased by 76% compared to that of nontransgenic mice. Since this study measured the activities of both *Glxr1* and *Glxr2*, the result did not reflect the net increase of *Glxr2* activity in heart mitochondria. To further understand the extent of *Glxr2* overexpression in heart of transgenic mice, total *Glxr* activity in homogenates of isolated heart mitochondria was determined. As shown in Fig. 1E, *Glxr* activity in heart mitochondria of nontransgenic mice was barely detectable ( $1.44 \pm 0.74$  nmol NADPH/min/mg protein), and expression of the human *Glxr2* transgene in cardiomyocytes led to a 53 fold increase in *Glxr* activity ( $77.68 \pm 23.51$  nmol NADPH/min/mg protein) in heart mitochondria of *Glxr2* transgenic mice.

Finally, we determined whether an increase in *Glxr2* activity in heart of transgenic mice affects the expression of other antioxidant enzymes. As shown in Fig. 1F, the protein levels of CuZnSOD, MnSOD, catalase, and Trx2 were unchanged in hearts of *Glxr2* transgenic mice

compared to those of their nontransgenic littermates. Furthermore, the activities of glutathione peroxidase were equivalent in whole heart homogenates of nontransgenic and *Glxr2* transgenic mice ( $9.46 \pm 0.97$  vs.  $8.69 \pm 0.92$  nmol NADPH/min/mg protein, respectively;  $p=0.185$ ,  $n=6$ ). However, the protein level of *Glxr1* was increased by 109% ( $p<0.001$ ) in heart of *Glxr2* transgenic mice relative to that of nontransgenic littermates (Fig. 1F). Finally, because all the antibodies commercially available only react with the human thioredoxin 1 (Trx1) but not the corresponding mouse protein, we were not able to measure its level of expression in mouse heart.

### 3.2. Overexpression of *Glxr2* protects mouse heart against DOX-induced mitochondrial dysfunction

Mitochondrion is the major subcellular organelle for generation of ROS in DOX-poisoned hearts and therefore a direct target of oxidative stress [7–9,13–19]. To investigate the effect of *Glxr2* overexpression on DOX-induced cardiac toxicity, we measured the efficiency of mitochondrial respiration in mouse hearts isolated from nontransgenic and *Glxr2* transgenic mice at days 1 and 5 of treatment with saline (as control) or DOX. As shown in Figs. 2 through 4, the baseline values of mitochondrial respiration including the rates of state 3 and 4 respiration, RCR, and P/O ratio using either NAD- or FAD-linked substrates were equivalent in saline-treated nontransgenic and *Glxr2* transgenic mice, indicating that overexpression of *Glxr2* has no effect on the efficiency of mitochondrial respiration in mouse heart under normal physiological conditions.

However, at one day after DOX treatment, the rate of NAD-linked state 3 respiration but not state 4 respiration was decreased by 36% in heart mitochondria of nontransgenic mice compared to those of saline-treated counterparts (Fig. 2A and B), leading to a 31% decrease

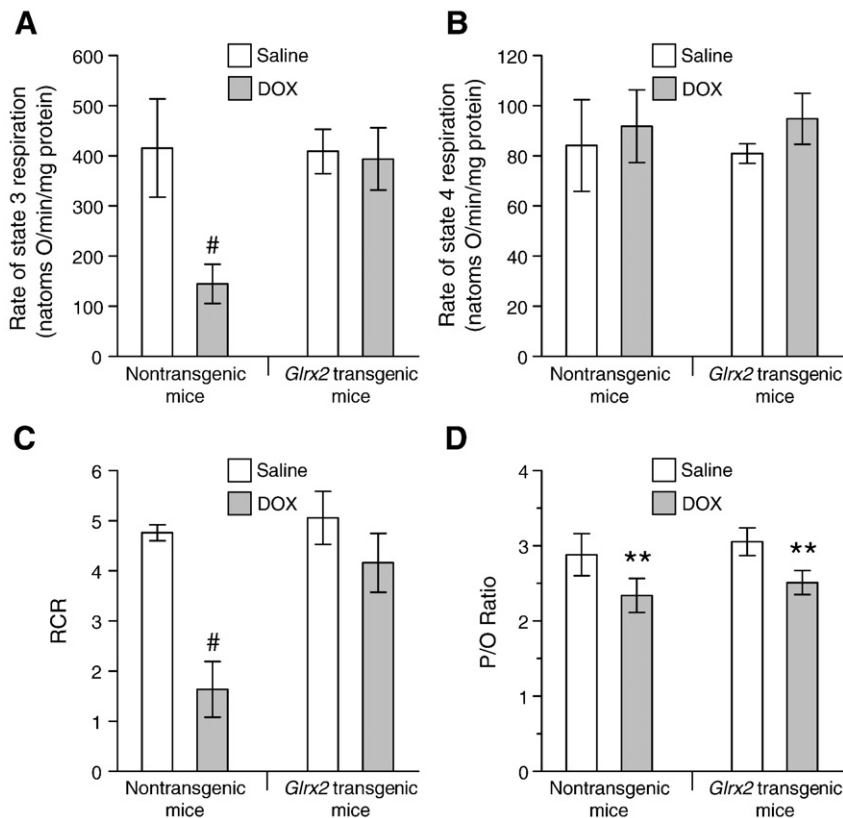


**Fig. 3.** *Glxr2* overexpression attenuates DOX-induced decrease in the efficiency of NAD-linked respiration in heart mitochondria at day 5 of treatment. In (A) and (C), DOX treatment greatly decreases the rate of state 3 respiration and RCR in heart mitochondria of nontransgenic mice but not littermate *Glxr2* transgenic mice. (B) The rate of state 4 respiration is not changed following DOX treatment in either type of mice. (D) *Glxr2* overexpression does not attenuate DOX-induced decrease in P/O ratio. Each bar represents mean  $\pm$  SD and  $n=6$  for each experiment. \*\* $p<0.01$ , and #,  $p<0.001$  versus heart mitochondria of saline-treated mice with of the same genotype.

in RCR (Fig. 2C). These results suggest that the rate of ATP synthesis using NAD-linked substrates in heart mitochondria of nontransgenic mice is retarded due to DOX treatment. Remarkably, overexpression of mitochondrial *Glxr2* completely prevented the functional abnormalities of heart mitochondria as a result of DOX treatment (Fig. 2A and C). On the other hand, the P/O ratio of all mitochondrial samples was not affected by DOX at day 1 of treatment (Fig. 2D), suggesting that the mitochondrial electron transport chain is still tightly coupled to oxidative phosphorylation. Furthermore, DOX treatment had no effect on FAD-linked respiration in heart mitochondria of either nontransgenic or *Glxr2* transgenic mice (data not shown).

DOX had a more profound impact on mitochondrial respiration at day 5 of treatment. As shown in Fig. 3A and C, heart mitochondria of nontransgenic mice exhibited 65% and 66% decreases in NAD-linked state 3 respiration and RCR, respectively, compared to saline-treated counterparts. Again, these functional derangements of mitochondria could be completely prevented by *Glxr2* overexpression (Fig. 3A and C). In addition, the P/O ratio of heart mitochondria from DOX-treated nontransgenic mice was decreased by 19% relative to the control level (Fig. 3D). Since the rate of state 4 respiration is not altered by DOX treatment (Fig. 3B), a decrease in P/O ratio suggests that electron transport in the respiratory chain is partially uncoupled from oxidative phosphorylation. To our surprise, this defect was not preventable by *Glxr2* overexpression (Fig. 3D).

While DOX at day 1 of treatment did not affect FAD-linked respiration in heart mitochondria of either type of mice, it did at day 5 of treatment. As shown in Fig. 4A through C, while the rate of FAD-linked state 4 respiration remained unchanged in DOX-treated nontransgenic mice, the rate of state 3 respiration was decreased by 27% compared to that of controls, resulting in a 19% decrease in RCR. The observed declines in mitochondrial respiration could also be

completely prevented by overexpression of *Glxr2* in transgenic hearts. DOX treatment also caused a decrease in P/O ratio of heart mitochondria isolated from either type of mice (Fig. 4D). Although the magnitude of decrease in heart mitochondria of *Glxr2* transgenic mice is less than that of nontransgenic mice (14% vs. 27%, respectively), the difference is not statistically significant, suggesting that an enhanced expression of *Glxr2* is not capable of ameliorating DOX-induced uncoupling of the electron transport chain in mitochondrial respiration that uses FAD-linked substrate.

### 3.3. *Glxr2* overexpression prevents DOX-induced release of creatine kinase from heart into circulation

Elevated level of creatine kinase in serum has been used as a marker for determining the extent of heart injury in mice treated with DOX [25,26]. As shown in Fig. 5A, the serum level of creatine kinase was not changed in both types of mice at day 1 of DOX treatment. However, at day 5 of DOX treatment, there was an approximately 500% increase in the level of serum creatine kinase in nontransgenic mice but not in *Glxr2* transgenic mice compared to their saline-treated counterparts (Fig. 5B). These data support the role of *Glxr2* in cardioprotection against DOX toxicity. Furthermore, since *Glxr2* is specifically overexpressed in hearts of transgenic mice, our results indicate that heart is the major organ that releases creatine kinase into the circulation due to DOX toxicity.

### 3.4. *Glxr2* overexpression prevents DOX-induced decline in left ventricular function

We next determined whether overexpression of *Glxr2* also protects mouse heart from DOX-induced decline in left ventricular

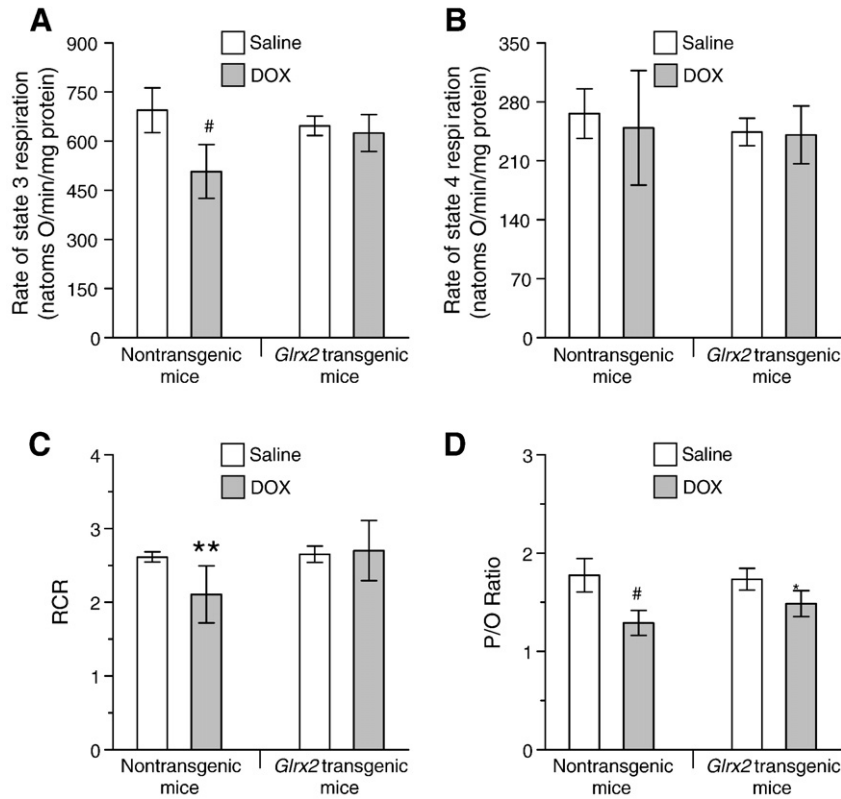


**Fig. 4.** *Glrx2* overexpression attenuates DOX-induced decrease in the efficiency of FAD-linked respiration in heart mitochondria at day 5 of treatment. In (A) and (C), FAD-linked state 3 respiration and RCR are decreased in heart mitochondria of nontransgenic mice but not littermate *Glrx2* transgenic mice treated with DOX. (B) The rate of state 4 respiration is not affected by DOX treatment in either type of mice. (D) *Glrx2* overexpression does not attenuate DOX-induced decrease in P/O ratio. Each bar represents mean±SD and  $n=6$  for each experiment. \* $p<0.05$ , \*\* $p<0.01$ , and #  $p<0.001$  versus heart mitochondria of saline-treated mice of the same genotype.

function. Previous studies have shown that the contractile function of mouse heart is not affected at one day after DOX treatment (data not shown). We therefore measured the *in vivo* cardiac function of nontransgenic and *Glrx2* transgenic mice at 5 days after DOX treatment. As shown in Table 1, there were no differences in the body weight and cardiac function between nontransgenic and *Glrx2* transgenic mice receiving treatment of saline, indicating that overexpression of mitochondrial *Glrx2* has no effect on the basal hemodynamic indices of mouse heart. However, the left ventricular contractile function was significantly depressed in DOX-

treated nontransgenic mice, as evidenced by a significant decrease in heart rate (29%), stroke index (SI) (36%), cardiac index (CI) (52%), ejection fraction (EF) (43%) and preload recruitable stroke work (PRSW) (61%) in comparison to those of saline-treated nontransgenic mice. DOX treatment also caused alterations in systolic function of nontransgenic hearts, including decreases in both end-systolic pressure ( $P_{es}$ ) and the maximal rate of pressure increasing ( $dP/dt_{max}$ ) and an increase in end-systolic volume ( $V_{es}$ ). The same was true for diastolic function of nontransgenic hearts, as shown by DOX-induced increases in end-diastolic pressure ( $P_{ed}$ ) and  $\tau$

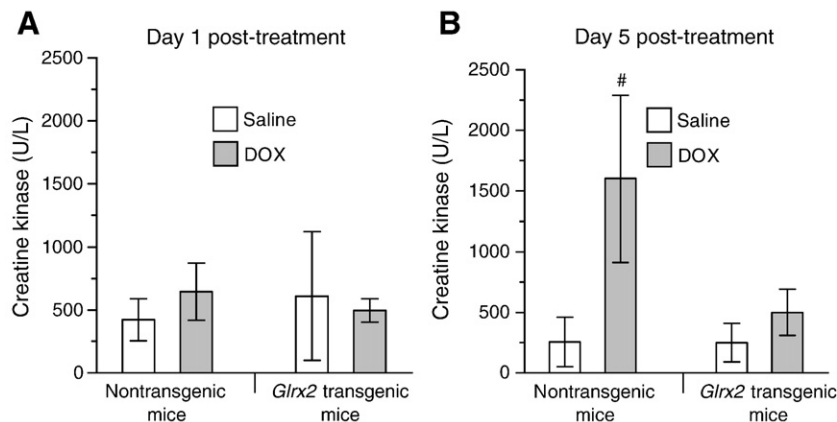


**Fig. 5.** *Glrx2* overexpression prevents DOX-induced increase in serum creatine kinase at day 5 of treatment. Blood was collected from mice via cardiac puncture at days 1 and 5 of treatment with saline or DOX and serum was then prepared. Each bar represents mean±SD and  $n\geq 5$ . #,  $p<0.001$  versus saline-treated nontransgenic mice.

**Table 1**

*In vivo* cardiac function of nontransgenic and *Glrx2* transgenic mice at day 5 of treatment with either saline or DOX

Parameter	Nontransgenic mice		<i>Glrx2</i> Transgenic mice	
	Treatment		Treatment	
	Saline	DOX	Saline	DOX
Body weight (grams)	28.20±3.62	22.60±2.16*	26.50±1.98	23.00±2.47‡
Heart rate (beats/min)	537±37	383±101**	537±51	487±47
SI (μl/g)	0.44±0.06	0.28±0.04**	0.47±0.06	0.40±0.06
CI (μl/g)	231±20	111±26**	250±37	194±29‡
EF (%)	69.40±2.06	39.40±6.56**	69.50±2.40	56.10±3.30‡
PRSW (mmHg)	97.10±14.27	37.90±13.70**	95.50±15.98	79.20±20.91
Systolic function				
P <sub>es</sub> (mmHg)	92.40±7.80	57.30±5.98**	93.00±5.53	82.30±10.95
V <sub>es</sub> (μl)	5.74±0.44	10.24±1.84**	5.97±0.92	7.54±0.65‡
dP/dt <sub>max</sub> (mmHg/s)	10714±1672	4861±1210**	9934±1404	9869±2611
dP/dt <sub>max</sub> -V <sub>ed</sub> (mmHg/μl)	764±217	302±133**	705±358	778±364
Diastolic function				
P <sub>ed</sub> (mmHg)	3.82±0.34	5.16±0.93**	3.91±0.78	2.86±1.10
V <sub>ed</sub> (μl)	17.06±1.18	15.46±1.36*	17.07±0.43	15.69±0.42‡
dP/dt <sub>min</sub> (mmHg/s)	10899±1857	3772±922**	10911±1268	8814±931‡
τ (Weiss) (ms)	5.67±0.55	10.15±2.67**	5.80±0.61	6.34±0.76
β(beta) (mmHg/μl)	0.32±0.07	0.35±0.22	0.36±0.18	0.28±0.22
Vascular function				
E <sub>a</sub> (mmHg/μl)	7.43±0.70	9.35±1.45*	7.65±0.69	9.11±1.14‡

SI, stroke index (SI=stroke volume/body weight); CI, cardiac index (CI=cardiac output/body weight); EF, ejection fraction; PRSW, preload recruitable stroke work; P<sub>es</sub>, end-systolic pressure; V<sub>es</sub>, end-systolic volume; dP/dt<sub>max</sub>, the maximal rate of pressure increasing; dP/dt<sub>max</sub>-V<sub>ed</sub>, slope describing isovolumic contraction; P<sub>ed</sub>, end-diastolic pressure; V<sub>ed</sub>, end-diastolic volume; dP/dt<sub>min</sub>, the maximal rate of pressure decreasing; τ (Weiss), time constant of isovolumic relaxation; β, slope of end-diastolic pressure–volume relationship; E<sub>a</sub>, arterial elastance. Each value represents mean±SD of 6 hearts. \*, *p*<0.05 versus saline-treated nontransgenic mice and saline-treated *Glrx2* transgenic mice; \*\*, *p*<0.05 versus saline-treated nontransgenic mice and *Glrx2* transgenic mice treated with either saline or DOX; ‡, *p*<0.05 versus saline-treated *Glrx2* transgenic mice.

(tau, time constant of isovolumic relaxation) as well as decreases in end-diastolic volume (V<sub>ed</sub>) and the maximal rate of pressure decreasing (dP/dt<sub>min</sub>).

Overexpression of mitochondrial *Glrx2* in the heart completely prevented DOX-induced changes in many hemodynamic parameters including heart rate, SI, PRSW, systolic function (P<sub>es</sub> and dP/dt<sub>max</sub>), and diastolic function (P<sub>ed</sub> and τ); and greatly attenuated the alterations in other functional measurements such as CI, EF, V<sub>es</sub> of systolic function, and dP/dt<sub>min</sub> of diastolic function compared to those of DOX-treated nontransgenic mice. These results demonstrate the function of mitochondrial *Glrx2* in protecting heart from DOX-induced contractile dysfunction.

On the other hand, the decrease in end-diastolic volume (V<sub>ed</sub>) due to DOX treatment was not preventable by *Glrx2* overexpression. In addition, *Glrx2* overexpression did not attenuate DOX-induced loss of body weight, indicating that cardiac injury resulting from DOX toxicity is not a cause of this phenotypic change. Finally, the extent of increase in peripheral vascular resistance (or arterial elastance, E<sub>a</sub>) due to DOX treatment was also not affected by an enhanced expression of *Glrx2*. This result is anticipated. Since *Glrx2* is only overexpressed in cardiomyocytes, it should not have an effect on DOX-induced increase in peripheral vascular resistance.

### 3.5. *Glrx2* overexpression attenuates cytochrome *c* release from heart mitochondria in response to tBid

Having established the protective role of *Glrx2* in DOX toxicity, we intended to investigate the mechanisms by which mitochondrial *Glrx2* limits DOX-induced myocardial injury. DOX-induced cardiomyopathy *in vivo* in mouse heart is partly mediated through apoptosis, as evidenced by the appearance of the typical apoptotic morphology in cardiomyocytes as well as a marked increase in

apoptotic effectors such as activated caspase 3 and cytosolic cytochrome *c* in DOX-poisoned hearts [18,57–59]. We therefore determined whether overexpression of *Glrx2* affected the release of cytochrome *c* from heart mitochondria in response to iBid, the proteolytically cleaved product of Bid functioning in promoting apoptosis [60]. As shown in Fig. 6A, heart mitochondria could maintain the integrity of their membranes *in vitro* even after 2 h incubation in the experimental buffer (as evidenced by the absence of cytochrome *c* release into supernatant). However, inclusion of either a 26-mer synthetic peptide encompassing the BH3 domain of Bid or a recombinant mouse tBid in the experimental buffer caused an extensive release of cytochrome *c* from heart mitochondria of a nontransgenic mouse, with levels plateauing at 1 h of incubation (Fig. 6A and B). Remarkably, overexpression of *Glrx2* in heart mitochondria greatly attenuated the extent of cytochrome *c* release in response to the same treatments.

### 3.6. *Glrx2* overexpression enhances *S*-glutathionylation of heart mitochondrial proteins

We next investigated the effect of *Glrx2* overexpression on protein *S*-glutathionylation in heart mitochondria, since *Glrx* can catalyze both de-glutathionylation and *S*-glutathionylation of proteins [37,42–44]. As shown in Fig. 7A, the extent of *S*-glutathionylation of several mitochondrial proteins in *Glrx2* transgenic hearts was increased compared to that of nontransgenic hearts. It is worth noting that because the cysteine residues of these mitochondrial proteins are *S*-glutathionylated and may also be alkylated with NEM, the molecular masses of these proteins cannot be estimated using gel electrophoresis in which the commercially available protein markers, that have been reduced with dithiothreitol, are used as standards. Further studies showed that these mitochondrial proteins of nontransgenic hearts also became more prominently *S*-glutathionylated at day 5 of DOX treatment, to a level higher than that of saline-treated nontransgenic mice but below that found in saline-treated *Glrx2* transgenic mice (Fig. 7B). DOX treatment further enhanced the extent of

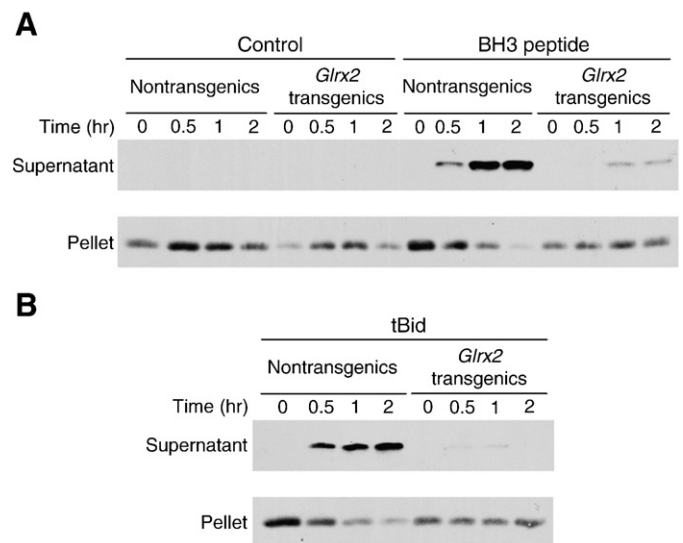


**Fig. 6.** Attenuation of tBid-induced cytochrome *c* release from heart mitochondria by *Glrx2*. (A) Representative protein blot analysis (from a total of four independent experiments) of cytochrome *c* in pellets and supernatants of heart mitochondria of a nontransgenic mouse and a *Glrx2* transgenic littermate in the absence or presence of 50 μM BH3 peptide of Bid. (B) Representative protein blot study showing that heart mitochondria from a *Glrx2* transgenic mouse release less cytochrome *c* than do heart mitochondria of a nontransgenic littermate following incubation with 1 μM of recombinant mouse tBid.



protein S-glutathionylation in heart mitochondria of *Glrx2* transgenic mice compared to that of the same mice treated with saline.

#### 4. Discussion

Generation of ROS by DOX via the formation of a complex with iron (III) and by the redox cycling reaction in cardiomyocytes is believed to initiate a cascade of oxidative chain reactions that eventually leads to the observed acute and chronic cardiotoxicity of DOX. Since iron(III) may be present in all cellular compartments and the enzymes responsible for redox cycling of DOX are located in the cytosol and several subcellular organelles of cardiomyocytes [7–12], ROS are likely to be generated throughout the entire cardiomyocyte. Whether the oxidants generated in each of the subcellular compartments contribute equally to DOX-induced cardiac injury is not understood. However, previous studies have suggested that mitochondria are both the primary subcellular site for generation of ROS and target of oxidative stress in DOX-poisoned hearts [7–9,16,17,19,25,61]. Since mitochondria play a major role in maintenance of normal cell metabolic function and in the control of apoptosis [62], a decrease in mitochondrial function as a result of oxidative damage often leads to cell injury and potentially cell death. This hypothesis is supported by an earlier study that cardiac overexpression of MnSOD effectively attenuates DOX-induced toxicity [25]. The current study further supports the mitochondrial hypothesis of DOX-induced cardiotoxicity by showing the protective function of another mitochondrial protein – *Glrx2* which catalyzes both de-glutathionylation and S-glutathionylation of proteins.

Our studies show that despite a decrease in efficiency of mitochondrial respiration at day 1 of DOX treatment in nontransgenic

mice (Fig. 2), the left ventricular function of these mice remains normal. Contractile dysfunction was only found at day 5 of DOX treatment when structural damage, including formation of intracytoplasmic vacuoles, extensive cell apoptosis and necrosis, and disarray of myofilaments, was evident [4,15,18,25,57,58]. These understandings suggest that derangement of mitochondrial respiration may serve as an early marker for DOX-induced cardiotoxicity, prior to when structural and contractile abnormalities are apparent. However, whether mitochondrial dysfunction directly contributes to the other pathological changes found in DOX-poisoned hearts remains to be determined.

The present study indicates the role of *Glrx2* in preventing DOX-induced cardiac injury. How does *Glrx2* protect heart from DOX toxicity? There are two potential mechanisms. First, as shown in Fig. 1E, overexpression of *Glrx2* also induces the expression of the endogenous mouse *Glrx1*, the cytosolic isoform of *Glrx*, in the heart. Therefore, it is possible that the observed protective function of *Glrx2* is mediated through an enhanced expression of *Glrx1*. However, heart mitochondria of *Glrx1* transgenic mice with cardiac overexpression of *Glrx1* (>20 fold increase in *Glrx1* protein) are not protected from DOX-induced dysfunction, suggesting that *Glrx1* plays a very limited role in cardioprotection against DOX treatment ([63], Ho et al., unpublished data). Second, a recent study indicates that *Glrx2* also exhibits GSH-dependent as well as thioredoxin reductase-dependent peroxidase activities [64]. This raises the possibility that the cardioprotective function of *Glrx2* may lie in its catalytic activity of peroxidase but not de-glutathionylation/S-glutathionylation, since overexpression of *Gpx1* in mouse heart is known to attenuate the cardiac toxicity of DOX [27]. We therefore measured the activity of glutathione peroxidase (*Gpx*) in isolated heart mitochondria of

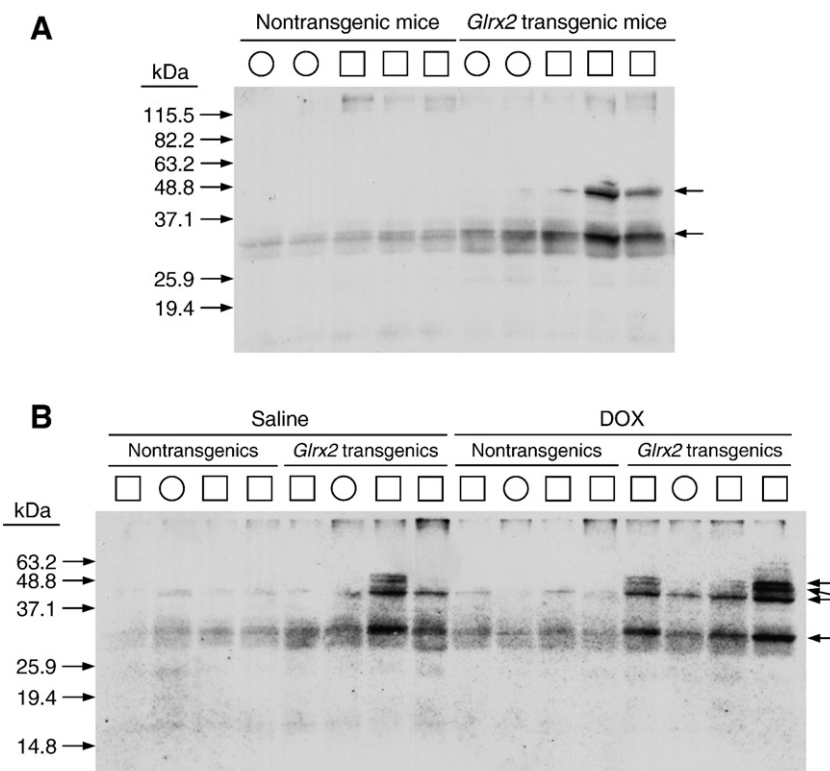


**Fig. 7.** *Glrx2* overexpression and DOX treatment increase S-glutathionylation of heart mitochondrial proteins. (A) S-glutathionylation of mitochondrial proteins in hearts of nontransgenic mice and *Glrx2* transgenic mice under normal physiological conditions. Forty micrograms of soluble mitochondrial proteins were separated on a 11% SDS-gel without the use of reducing agent ( $\beta$ -mercaptoethanol) for blot analysis using an anti-GSH antibody. (B) Detection of S-glutathionylated mitochondrial proteins in hearts of nontransgenic mice and *Glrx2* transgenic mice at day 5 of treatment with either saline or DOX. In (A and B), square and circle represent male and female mice, respectively. The most prominently S-glutathionylated proteins are indicated by arrows on the right. The positions where the reduced protein standards migrate are indicated on the left. A duplicate gel loaded with the same amounts of samples was stained with Coomassie Brilliant Blue to ensure equal loading of the samples (data not shown).

nontransgenic and *Glrx2* transgenic mice. The Gpx activities in the former and latter samples are equivalent ( $13.63 \pm 3.72$  vs.  $14.14 \pm 5.01$  nmol NADPH/min/mg protein, respectively;  $p=0.83$ ,  $n \geq 6$ ), suggesting that the contribution of the overexpressed *Glrx2* to total GSH-dependent peroxidase activity in heart mitochondria is negligible, therefore excluding the Gpx activity of *Glrx2* in cardioprotection. This result is not surprising since the catalytic efficiency of GSH-dependent peroxidase of the human *Glrx2* protein ( $2.5 \times 10^4 \text{ s}^{-1} \text{ M}^{-1}$ ) is significantly lower than that of Gpx ( $\sim 10^8 \text{ s}^{-1} \text{ M}^{-1}$ ) [64]. Furthermore, in contrast to the results of Fernando et al. [64], we failed to observe an increase in thioredoxin reductase-dependent peroxidase activity in heart mitochondria of *Glrx2* transgenic mice compared to that of nontransgenic mice ( $6.15 \pm 1.60$  vs.  $5.81 \pm 1.66$  nmol NADPH/min/mg protein, respectively;  $p=0.70$ ,  $n \geq 6$ ). These results rule out the roles of the endogenous mouse *Glrx1* as well as the associated peroxidase activities of *Glrx2* in preventing DOX-induced cardiac injury.

DOX treatment has been shown to induce apoptosis *in vivo* in hearts of rodents as well as *in vitro* in cultured cardiomyocytes [17,18,57–59]. However, whether death of cardiomyocytes by apoptosis directly contributes to DOX-induced myocardial injury and declines in left ventricular function as observed in the experimental animals and cancer patients is not known. Our studies show that heart mitochondria overexpressing *Glrx2* are more resistant to tBid-induced release of cytochrome *c*, an initiator of the post-mitochondrial pathway of apoptosis via formation of an apoptosome with Apaf-1 (apoptotic protease activating factor 1) [65]. Although these results suggest that the increased tolerance of heart mitochondria of *Glrx2* transgenic mice to tBid-mediated apoptosis renders the mice more resistant to DOX-induced cardiac toxicity, further studies to understand the role of apoptosis in DOX-induced myocardial injury, such as whether DOX treatment activates Bid in heart and whether *Glrx2* modulates apoptosis in DOX-poisoned cardiomyocytes, are needed.

*Glrx* is known to play a major role in modulating the extent of protein S-glutathionylation in mammalian cells by catalyzing both the reduction and formation of protein–SSG mixed disulfides. The mechanism of *Glrx*-catalyzed protein S-glutathionylation is not completely understood. However, it should be noted that the S-glutathionylation activity of *Glrx1* and *Glrx2* has only been demonstrated *in vitro* in reactions where purified proteins and mitochondrial membrane are incubated with recombinant *Glrx* proteins [42–44]. Whether this reaction also occurs *in vivo* is not known. To date, overexpression of *Glrx1* in cultured cells has always been found to cause to an enhanced activity in removal of the glutathionyl moiety in several proteins such as Ras, the inhibitory  $\kappa\text{B}$  kinase  $\beta$  (IKK- $\beta$ ), and procaspase 3 [36,66,67]; and down-regulation of *Glrx1* by RNA interference retards the rate of de-glutathionylation of S-glutathionylated actin, procaspase 3, and IKK- $\beta$  [66–68]. There is only one study which provides indirect evidence to suggest that *Glrx1* promotes S-glutathionylation of the p65 subunit of NF- $\kappa\text{B}$  in a line of pancreatic carcinoma cells exposed to both hypoxia and N-acetyl-L-cysteine [69]. The current study for the first time demonstrates that an enhanced expression of *Glrx2* increases S-glutathionylation of heart mitochondrial proteins, and this is associated with tolerance of heart to the toxicity of DOX. These results suggest that S-glutathionylation of a limited number of heart mitochondrial proteins plays a role in preventing DOX-induced mitochondrial dysfunction and the subsequent contractile abnormalities in heart. Future studies to identify these S-glutathionylated mitochondrial proteins and to determine the significance of protein S-glutathionylation in the cardioprotective function of *Glrx2* should further our understanding in the biochemical mechanisms of DOX-induced cardiac injury.

Finally, our studies implicate the role of *Glrx2* in protecting the mitochondrial electron transport chain from DOX-induced damage. As shown in Figs. 2 through 4, the rate of NAD-linked but not FAD-linked state 3 respiration is decreased in heart mitochondria of nontransgenic mice at one day after DOX treatment. Since the NAD-linked

respiration is carried out by complexes I, III and IV of the electron transport chain and FAD-linked respiration uses complexes II, III and IV, the observed decline in NAD-linked respiration is believed to result from impairment of complex I activity, as also documented in several earlier studies [16,17,27,70]. In addition, DOX retards the rates of both NAD- and FAD-linked state 3 respiration at day 5 of treatment, suggesting that the activities of both complex I (for NAD-linked respiration) and II (for FAD-linked respiration) are decreased, and/or the activities of complexes III and/or IV are also affected. Most importantly, the DOX-induced declines in rate of state 3 respiration are completely absent in heart mitochondria of *Glrx2* transgenic mice, suggesting the function of *Glrx2* in preventing DOX-induced inactivation of the mitochondrial electron transport chain.

In summary, our results show that overexpression of *Glrx2* in heart mitochondria significantly prevents DOX-induced dysfunction of mitochondrial respiration, release of creatine kinase from cardiomyocytes into circulation, and decrease in left ventricular function. Furthermore, the observed cardioprotective function of *Glrx2* is associated with an increase in S-glutathionylation of heart mitochondrial proteins, suggesting that formation of protein–SSG mixed disulfides is actually protective. The protection may result from the altered catalytic/structural function of these S-glutathionylated mitochondrial proteins. Alternatively, S-glutathionylation may prevent a more drastic and irreversible modification, such as formation of sulfenic and sulfonic acids, of the cysteine residues in these proteins. Further research to understand the molecular mechanisms of cardioprotection by protein S-glutathionylation should allow identification of new pathways of DOX-induced cardiotoxicity that can be targeted therapeutically.

#### Acknowledgements

We are grateful to Dr. Jeff Robbins of University of Cincinnati for the gift of the plasmid containing the 5' flanking sequence and promoter of the mouse  $\alpha\text{-MyHC}$  gene, Dr. Chuan-Pu Lee of Wayne State University for lending us the equipment for measurement of mitochondrial respiration, and Drs. David C. S. Huang and Ruth Kluck of The Walter and Eliza Hall Institute of Medical Research, Victoria, Australia, for the information regarding the use of the peptide containing the BH3 domain of Bid.

#### References

- [1] V.J. Ferrans, Overview of cardiac pathology in relation to anthracycline cardiotoxicity, *Cancer Treat. Rep.* 62 (1978) 955–961.
- [2] K. Shan, A.M. Lincoff, J.B. Young, Anthracycline-induced cardiotoxicity, *Ann. Intern. Med.* 125 (1996) 47–58.
- [3] M.R. Bristow, P.D. Thompson, R.P. Martin, J.W. Mason, M.E. Billingham, D.C. Harrison, Early anthracycline cardiotoxicity, *Am. J. Med.* 65 (1978) 823–832.
- [4] P.K. Singal, N. Iliskovic, Doxorubicin-induced cardiomyopathy, *N. Engl. J. Med.* 339 (1998) 900–905.
- [5] J.L. Zweier, L. Gianni, J. Muindi, C.E. Myers, Differences in  $\text{O}_2$  reduction by the iron complexes of adriamycin and daunomycin: the importance of the sidechain hydroxyl group, *Biochem. Biophys. Acta* 884 (1986) 326–336.
- [6] K.L. Maliszka, B.B. Hasinoff, Production of hydroxyl radical by iron(III)-anthraquinone complexes through self-reduction and through reductive activation by the xanthine oxidase/hypoxanthine system, *Arch. Biochem. Biophys.* 321 (1995) 51–60.
- [7] J.H. Doroshow, Anthracycline antibiotic-stimulated superoxide, hydrogen peroxide, and hydroxyl radical production by NADH dehydrogenase, *Cancer Res.* 43 (1983) 4543–4551.
- [8] K.J. Davies, J.H. Doroshow, Redox cycling of anthracyclines by cardiac mitochondria. I. Anthracycline radical formation by NADH dehydrogenase, *J. Biol. Chem.* 261 (1986) 3060–3067.
- [9] J.H. Doroshow, K.J. Davies, Redox cycling of anthracyclines by cardiac mitochondria. II. Formation of superoxide anion, hydrogen peroxide, and hydroxyl radical, *J. Biol. Chem.* 261 (1986) 3068–3074.
- [10] N.R. Bachur, S.L. Gordon, M.V. Gee, H. Kon, NADPH cytochrome P-450 reductase activation of quinone anticancer agents to free radicals, *Proc. Natl. Acad. Sci. U. S. A.* 76 (1979) 954–957.
- [11] J. Vázquez-Vivar, P. Martasek, N. Hogg, B.B.S. Masters, K.A. Pritchard, B. Kalyanaram, Endothelial nitric oxide synthase-dependent superoxide generation from Adriamycin, *Biochemistry* 36 (1997) 11293–11297.

- [12] A.P. Garner, M.J.I. Paine, I. Rodriguez-Crespo, E.C. Chinje, P.O. Ortiz De Montellano, I.J. Stratford, D.G. Tew, C.R. Wolf, Nitric oxide synthases catalyze the activation of redox cycling and bioreductive anticancer agents, *Cancer Res.* 59 (1999) 1929–1934.
- [13] M. Praet, G. Pollakis, E. Goormaghtigh, J.M. Ruyschaert, Damages of the mitochondrial membrane in adriamycin treated mice, *Cancer Lett.* 25 (1984) 89–96.
- [14] L.E. Solem, T.R. Henry, K.B. Wallace, Disruption of mitochondrial calcium homeostasis following chronic doxorubicin administration, *Toxicol. Appl. Pharmacol.* 129 (1994) 214–222.
- [15] D.L. Santos, A.J. Moreno, R.L. Leino, M.K. Froberg, K.B. Wallace, Carvedilol protects against doxorubicin-induced mitochondrial cardiomyopathy, *Toxicol. Appl. Pharmacol.* 185 (2002) 218–227.
- [16] K.B. Wallace, Doxorubicin-induced cardiac mitochondriopathy, *Pharmacol. Toxicol.* 93 (2003) 105–115.
- [17] P.S. Green, C. Leeuwenburgh, Mitochondrial dysfunction is an early indicator of doxorubicin-induced apoptosis, *Biochim. Biophys. Acta* 1588 (2002) 94–101.
- [18] A. Ascensão, J. Magalhães, J.M. Soares, R. Ferreira, M.J. Neuparth, F. Marques, P.J. Oliveira, J.A. Duarte, Moderate endurance training prevents doxorubicin-induced *in vivo* mitochondriopathy and reduces the development of cardiac apoptosis, *Am. J. Physiol.: Heart Circ. Physiol.* 289 (2005) H722–H731.
- [19] P.J. Oliveira, M.S. Santos, K.B. Wallace, Doxorubicin-induced thiol-dependent alteration of cardiac mitochondrial permeability transition and respiration, *Biochemistry (Mosc)* 71 (2006) 194–199.
- [20] X. Liu, Z. Chen, C.C. Chua, Y.S. Ma, G.A. Youngberg, R. Hamdy, B.H.L. Chua, Melatonin as an effective protector against doxorubicin-induced cardiotoxicity, *Am. J. Physiol.: Heart Circ. Physiol.* 283 (2002) H254–H263.
- [21] N. Siveski-Illskovic, N. Kaul, P.K. Singal, Doxorubicin promotes endogenous antioxidants and provides protection against adriamycin-induced cardiomyopathy in rats, *Circulation* 89 (1994) 2829–2835.
- [22] C.F. Seifert, M.F. Nesser, D.F. Thompson, Dexrazoxane in the prevention of doxorubicin-induced cardiotoxicity, *Ann. Pharmacother.* 28 (1994) 1063–1072.
- [23] G.F. Samelis, G.P. Stathopoulos, D. Kotsarelis, I. Dontas, C. Frangia, P.E. Karayannacos, Doxorubicin cardiotoxicity and serum lipid increase is prevented by dexrazoxane (ICRF-187), *Anticancer Res.* 18 (1998) 3305–3309.
- [24] P. Nazeyrollas, A. Prevost, N. Baccard, L. Manot, P. Devillier, H. Millart, Effects of amifostine on perfused isolated rat heart and on acute doxorubicin-induced cardiotoxicity, *Cancer Chemother. Pharmacol.* 43 (1999) 227–232.
- [25] H.C. Yen, T.D. Oberley, S. Vichitbandha, Y.-S. Ho, D.K. Clair St, The protective role of manganese superoxide dismutase against adriamycin-induced acute cardiac toxicity in transgenic mice, *J. Clin. Invest.* 98 (1996) 1253–1260.
- [26] Y.J. Kang, Y. Chen, P.N. Epstein, Suppression of doxorubicin cardiotoxicity by overexpression of catalase in the heart of transgenic mice, *J. Biol. Chem.* 271 (1996) 12610–12616.
- [27] Y. Xiong, X. Liu, C.P. Lee, B.H.L. Chua, Y.-S. Ho, Attenuation of doxorubicin-induced contractile and mitochondrial dysfunction in mouse heart by cellular glutathione peroxidase, *Free Radical Biol. Med.* 41 (2006) 46–55.
- [28] A. Meister, M.E. Anderson, Glutathione, *Annu. Rev. Biochem.* 52 (1983) 711–760.
- [29] E. Pineda-Molina, P. Klatt, J. Vazquez, A. Marina, M.G. de Lacoba, D. Perez-Sala, S. Lamas, Glutathionylation of the p50 subunit of NF- $\kappa$ B: a mechanism for redox-induced inhibition of DNA binding, *Biochemistry* 40 (2001) 14134–14142.
- [30] S. Bandyopadhyay, D.W. Starke, J.J. Mielal, R.M. Gronostajski, Thioltransferase (glutaredoxin) reactivates the DNA-binding activity of oxidation-inactivated nuclear factor  $\kappa$ B, *J. Biol. Chem.* 273 (1998) 392–397.
- [31] W.C. Barrett, J.P. DeGnore, S. Konig, H.M. Fales, Y. Keng, Z. Zhong-Yin, M.B. Yim, P.B. Chock, Regulation of PTP1B via glutathionylation of the active site cysteine 215, *Biochemistry* 38 (1999) 6699–6705.
- [32] W.C. Barrett, J.P. DeGnore, Y. Keng, Z. Zhang, M.B. Yim, P.B. Chock, Roles of superoxide radical anion in signal transduction mediated by reversible regulation of protein-tyrosine phosphatase 1B, *J. Biol. Chem.* 274 (1999) 34543–34546.
- [33] N.E. Ward, J.R. Stewart, C.G. Ioannides, C.A. O' Brian, Oxidant-induced S-glutathionylation inactivates protein kinase C- $\alpha$  (PKC- $\alpha$ ): a potential mechanism of PKC isozyme regulation, *Biochemistry* 39 (2000) 10319–10329.
- [34] D.A. Davis, F.M. Newcomb, D.W. Starke, D.E. Ott, J.J. Mielal, R. Yarchoan, Thioltransferase (glutaredoxin) is detected within HIV-1 and can regulate the activity of glutathionylated HIV-1 protease *in vitro*, *J. Biol. Chem.* 272 (1997) 25935–25940.
- [35] A.L. Dafre, H. Sies, T. Akerboom, Protein S-thiolation and regulation of microsomal glutathione transferase activity by the glutathione redox couple, *Arch. Biochem. Biophys.* 332 (1996) 288–294.
- [36] T. Adachi, D.R. Pimentel, T. Heibeck, X. Hou, Y.L. Lee, B. Jiang, Y. Ido, R.A. Cohen, S-glutathionylation of Ras mediates redox-sensitive signaling by angiotensin II in vascular smooth muscle cells, *J. Biol. Chem.* 279 (2004) 29857–29862.
- [37] Y. Yang, S. Jao, S. Nanduri, D.W. Starke, J.J. Mielal, J. Qin, Reactivity of the human thioltransferase (glutaredoxin) C75, C255, C785, C825 mutant and NMR solution structure of its glutathionyl mixed disulfide intermediate reflect catalytic specificity, *Biochemistry* 37 (1998) 17145–17156.
- [38] W.W. Wells, Y. Yang, T.L. Deits, Z.R. Gan, Thioltransferases, *Adv. Enzymol. Relat. Areas Mol. Biol.* 66 (1993) 149–201.
- [39] M. Lundberg, C. Johansson, J. Chandra, M. Enoksson, G. Jacobsson, J. Ljung, M. Johansson, A. Holmgren, Cloning and expression of a novel human glutaredoxin (Grx2) mitochondrial and nuclear isoforms, *J. Biol. Chem.* 276 (2001) 26269–26275.
- [40] V.N. Gladyshev, A. Liu, S.V. Novoselov, K. Krysan, Q.A. Sun, V.M. Kryukov, G.V. Kryukov, M.F. Lou, Identification of a new mammalian glutaredoxin (thioltransferase), grx2, *J. Biol. Chem.* 276 (2001) 30374–30380.
- [41] S. Lind, R. Gerdes, I. Schuppe-Koistinen, I.A. Cotgreave, Studies on the mechanism of oxidative modification of human glyceraldehyde-3-phosphate dehydrogenase by glutathione: catalysis by glutaredoxin, *Biochem. Biophys. Res. Commun.* 247 (1998) 481–486.
- [42] D.W. Starke, P.B. Chock, J.J. Mielal, Glutathione-thiyl radical scavenging and transferase properties of human glutaredoxin (thioltransferase): Potential role in redox signal transduction, *J. Biol. Chem.* 278 (2003) 14607–14613.
- [43] S.M. Beer, E.R. Taylor, S.E. Brown, C.C. Dahm, N.J. Costa, M.J. Runswick, M.P. Murphy, Glutaredoxin 2 catalyzes the reversible oxidation and glutathionylation of mitochondrial membrane thiol proteins: implications for mitochondrial redox regulation and antioxidant defense, *J. Biol. Chem.* 279 (2004) 47939–47951.
- [44] E.B. Meyer, W.W. Wells, Thioltransferase increases resistance of MCF-7 cells to adriamycin, *Free Radical Biol. Med.* 26 (1999) 770–776.
- [45] C.A. Chrestensen, D.W. Starke, J.J. Mielal, Acute cadmium exposure inactivates thioltransferase (Glutaredoxin), inhibits intracellular reduction of protein-glutathionyl-mixed disulfides, and initiates apoptosis, *J. Biol. Chem.* 275 (2000) 26556–26565.
- [46] D. Daily, A. Vlamis-Gardikas, D. Offen, L. Mittelman, E. Melamed, A. Holmgren, A. Barzilai, Glutaredoxin protects cerebellar granule neurons from dopamine-induced apoptosis by activating NF- $\kappa$ B via Ref-1, *J. Biol. Chem.* 276 (2001) 1335–1344.
- [47] J.J. Song, J.G. Rhee, M. Suntharalingam, S.A. Walsh, D.R. Spitz, Y.L. Lee, Role of glutaredoxin in metabolic oxidative stress. Glutaredoxin as a sensor of oxidative stress mediated by H<sub>2</sub>O<sub>2</sub>, *J. Biol. Chem.* 277 (2002) 46566–46577.
- [48] H. Murata, Y. Ihara, H. Nakamura, J. Yodoi, K. Sumikawa, T. Kondo, Glutaredoxin exerts an antiapoptotic effect by regulating the redox state of Akt, *J. Biol. Chem.* 278 (2003) 50226–50233.
- [49] M. Enoksson, A.P. Fernandes, S. Prast, C.H. Lillig, A. Holmgren, S. Orrenius, Overexpression of glutaredoxin 2 attenuates apoptosis by preventing cytochrome c release, *Biochem. Biophys. Res. Commun.* 327 (2005) 774–779.
- [50] Z. Chen, C.C. Chua, Y.-S. Ho, R.C. Hamdy, B.H.L. Chua, Overexpression of Bcl-2 attenuates apoptosis and protects against myocardial I/R injury in transgenic mice, *Am. J. Physiol.: Heart Circ. Physiol.* 280 (2001) H2313–H2320.
- [51] A. Subramaniam, W.K. Jones, J. Gulick, S. Wert, J. Neumann, J. Robbins, Tissue-specific regulation of the  $\alpha$ -myosin heavy chain gene promoter in transgenic mice, *J. Biol. Chem.* 266 (1991) 24613–24620.
- [52] R. Hogan, F. Constantini, E. Lacy, Manipulating the mouse embryo: a laboratory manual, Cold Spring Harbor Laboratory, Cold Spring Harbor, (1986) 90–203.
- [53] P.S. Thomas, Hybridization of denatured RNA and small DNA fragments transferred to nitrocellulose, *Proc. Natl. Acad. Sci. U. S. A.* 77 (1980) 5201–5205.
- [54] C. Johansson, C.H. Lillig, A. Holmgren, Identification of a new mammalian glutaredoxin (thioltransferase), grx2, *J. Biol. Chem.* 279 (2004) 7537–7543.
- [55] C. Little, R. Olinescu, K.G. Reid, P.J. O'Brien, Properties and regulation of glutathione peroxidase, *J. Biol. Chem.* 245 (1970) 3632–3636.
- [56] N. Hosova-Matsuda, K. Motohashi, H. Yoshimura, A. Nozaki, K. Inoue, M. Ohmori, T. Hisabori, Anti-oxidative stress system in cyanobacteria. Significance of type II peroxidoredoxin and the role of 1-Cys peroxidoredoxin in *Synechocystis* sp. strain PCC 6803, *J. Biol. Chem.* 280 (2005) 840–846.
- [57] Y.J. Kang, Z.-W. Zhou, G.-W. Wang, A. Buridi, J.B. Klein, Suppression by metallothionein of doxorubicin-induced cardiomyocyte apoptosis through inhibition of p38 mitogen-activated protein kinases, *J. Biol. Chem.* 275 (2000) 13690–13698.
- [58] A. Childs, S.L. Phaneuf, A.J. Dirks, T. Phillips, C. Leeuwenburgh, Doxorubicin treatment *in vivo* causes cytochrome c release and cardiomyocyte apoptosis, as well as increased mitochondrial efficiency, superoxide dismutase activity, and Bcl-2:Bax ratio, *Cancer Res.* 62 (2002) 4592–4598.
- [59] R. Nithipongvanitch, W. Ittarat, J.M. Velez, R. Zhao, D.K. Clair St., T.D. Oberley, Evidence for p53 as guardian of the cardiomyocyte mitochondrial genome following acute adriamycin treatment, *J. Histochem. Cytochem.* 55 (2007) 629–639.
- [60] X. Luo, I. Budihardjo, H. Zou, C. Slaughter, X. Wang, Bid, a Bcl2 interacting protein, mediates cytochrome c release from mitochondria in response to activation of cell surface death receptors, *Cell* 94 (1998) 481–490.
- [61] L. Chaiswing, M.P. Cole, D.K. Clair St., W. Ittarat, L.I. Szveda, T.D. Oberley, Oxidative damage precedes nitrate damage in adriamycin-induced cardiac mitochondrial injury, *Toxicol. Pathol.* 32 (2004) 536–547.
- [62] D.R. Green, C. Kroemer, The pathophysiology of mitochondrial cell death, *Science* 305 (2004) 626–629.
- [63] G. Malik, N. Nagy, Y.-S. Ho, N. Maulik, D.K. Das, Role of glutaredoxin-1 in cardioprotection: an insight with Glrx1 transgenic and knockout animals, *J. Mol. Cell. Cardiol.* 44 (2008) 261–269.
- [64] M.R. Fernando, J.M. Lechner, S. Löfgren, V.N. Gladyshev, M.F. Lou, Mitochondrial thioltransferase (glutaredoxin 2) has GSH-dependent and thioredoxin reductase-dependent peroxidase activities *in vitro* and in lens epithelial cells, *FASEB J.* 20 (2006) 2645–2647.
- [65] P. Li, D. Nijhawan, I. Budihardjo, S.M. Srinivasula, M. Ahmad, E.S. Alnemri, X. Wang, Cytochrome c and dATP-dependent formation of Apaf-1/caspase-9 complex initiates an apoptotic protease cascade, *Cell* 91 (1997) 479–489.
- [66] N.L. Reynaert, A. van der Vliet, A.S. Guala, T. McGovern, M. Hristova, C. Pantano, N. H. Heintz, J. Heim, Y.-S. Ho, d.E. Matthews, E.F.M. Wouters, Y.M.W. Janseen-Heininger, Dynamic redox control of NF- $\kappa$ B through glutaredoxin-regulated S-glutathionylation of inhibitory  $\kappa$ B kinase, *Proc. Natl. Acad. Sci. U. S. A.* 103 (2006) 10386–10391.

- [67] S. Pan, B.C. Berk, Glutathiolation regulates tumor necrosis factor- $\alpha$ -induced caspase-3 cleavage and apoptosis: key role for glutaredoxin in the death pathway, *Circ. Res.* 100 (2007) 213–219.
- [68] J. Wang, E. Tekle, H. Outrahim, J.J. Mieyal, E.R. Stadtman, P.B. Chock, Stable and controllable RNA interference: investigating the physiological function of glutathionylated actin, *Proc. Natl. Acad. Sci. U. S. A.* 100 (2003) 5103–5106.
- [69] S. Qanungo, D.W. Starke, H.V. Pai, J.J. Mieyal, A.L. Nieminen, Glutathione supplementation potentiates hypoxic apoptosis by S-glutathionylation of p65-NF $\kappa$ B, *J. Biol. Chem.* 228 (2007) 18427–18436.
- [70] H.C. Yen, T.D. Oberley, C.G. Gairola, L.I. Szweda, D.K. Clair St, Manganese superoxide dismutase protects mitochondrial complex I against adriamycin-induced cardiomyopathy in transgenic mice, *Arch. Biochem. Biophys.* 362 (1999) 59–66.